Automatic Control of Arc Welding by Monitoring Molten Pool†

Yoshiaki ARATA* and Katsunori INOUE**

Abstract

In order to control arc welding automatically, a new monitoring method is developed. In this method, a flow of molten metal in a weld pool is observed using an electro-optical sensor and a logic circuit, and the physical position of the molten pool is measured. Static and dyaamic properties of this measured value is studied experimentally, and process variables that are necessary to compose an automatic control system are obtained from these properties. Some experiments on the automatic control system are carried out for the purpose of verifying correctness of this monitoring method and these process variables. Their results are satisfactory.

1. Introduction

In the existing feedback control system for arc welding, penetration is selected as a controlled variable in most cases.[1)~5)] Undoubtedly, penetration is an important factor and weld quality is frequently appraised based on this variable. However, for arc welding, enough penetration is a necessary but not sufficient condition.

For example, in narrow gap welding, a satisfactory result can not be obtained without complete building-up by filler metal even if enough penetration is achieved. In such case, the height, width and appearence of building-up must be monitored by any means. Besides, there are a number of difficulties in the sensing technique for penetration. In the use of an infra-red radiation pyrometer, the local differences of the surface emissibity of the work piece caused an error in penetration sensing. A conventional thermocouple technique has the weak points common to the other contact type sensing methods.

On the other hand, in order to compose a multi-variable feedback control system, it is necessary to establish two or more controlled variables. In such system, penetration must be controlled together with the other variables. Therefore, it is significant to establish a new controlled variables in a feedback control system of arc welding.

Authors developed a new method to sense a new controlled variable and investigated in this variable to establish the method. In this method, a molten pool is sighted with a specially designed camera, which consists of a simple optical system, from the back side during arc welding, and the image of the molten pool is projected on the focussing screen of the camera by a strong light of welding arc.

The physical position of the image and its momently change are converted into an electrical signal by the photoelectric elements installed on the screen.

Such a sensed signal corresponds to the building up of the deposited metal after weld has been finished and weld bead of uniform height can be maintained in a feedback control of this signal.

To compose an optimum feedback control system, the properties of a controlled system in connection with the each controlled variable should be clarified. Static and dynamic properties of the building-up of the deposited metal were obtained experimentally on utilizing above mentioned technique. And theoretical considerations on such properties were made.

Feedback control experiments were also made to verify these properties with an automatic control welder of prototype. A manipulated variable which acts on a controlled system is restricted to welding speed only throughout this study, but generality is not lost, because the same technique as described in this report can be applied to the case where a different manipulated variable is utilized.

2. Controlled variable and its sensing method

2-1 Principle

Figure 1 shows the illustrative principle of the controlled variable sensing method. The specially designed camera which is interlinked to a welder and travels with it sights the molten pool from the back side of arc during welding. A strong light emitted from arc projects the image of the molten pool on the focussing screen of the camera.

A typical pattern of the projected image on the

† Received on May 31, 1972

* Professor

** Research Associate, Dep. of Welding Engineering, Faculty of Engineering, Osaka University

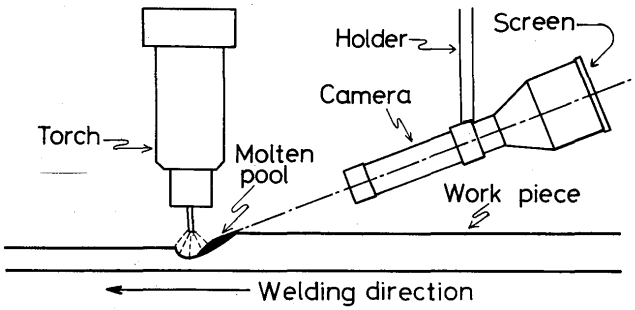

Fig. 1. Principle of the sensing method.

screen is shown in **Fig. 2** and **Photo. 1.** A bright part in the figures is an image of arc and lower part is intercepted by the molten pool that is a dark part. **Figures 3 (a)** and **(b)** show this aspect.

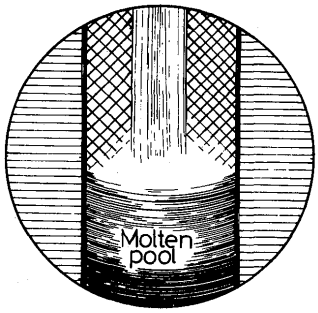

Fig. 2. Typical pattern of the image.

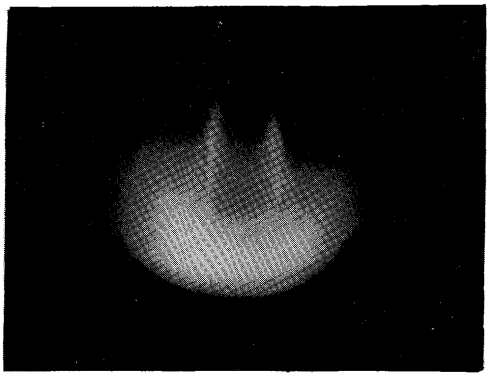

Photo. 1. Typical pattern of the image.

If the molten pool changes its physical position from a solid line to a broken line in these figures, the image also shifts upward on the screen. The shift length is proportional to $\Delta h \cdot \cos\varphi$. (for Δh and φ, refer to **Fig. 3 (b)**).

On the assumption that the physical position of the molten pool at a certain time, i. e. the height of the molten pool from a certain datum line, monistically corresponds to the deposited height of the filler metal at that time, the building up of the deposited metal can be measured by sensing the position of the borders of a bright and dark parts in the projected image.

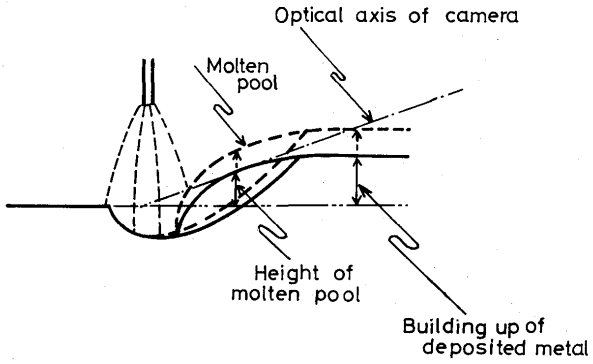

(a) Direct and indirect sensed variables.

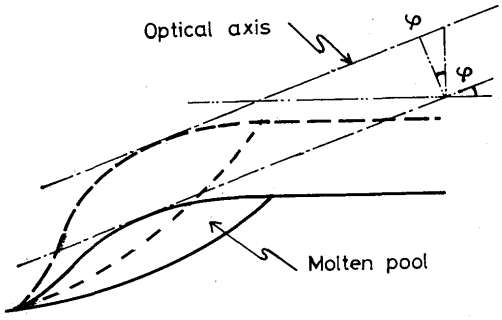

(b) A change of the sensed variable.

Fig. 3.

2-2 Sensing method

The border position of the image is sensed by the twenty photoelectric elements (silicon-photo-diode) which are arranged in a column on the focussing screen of the camera as shown in **Fig. 4.** All the photoelectric elements have their serial number in order of the position for convenience's sake and are connected to the logic circuit whose block diagram is shown in **Fig. 5 (a).** Each of twenty photoelectric elements is connected to the voltage comparator of the same serial number. The output terminal of a certain

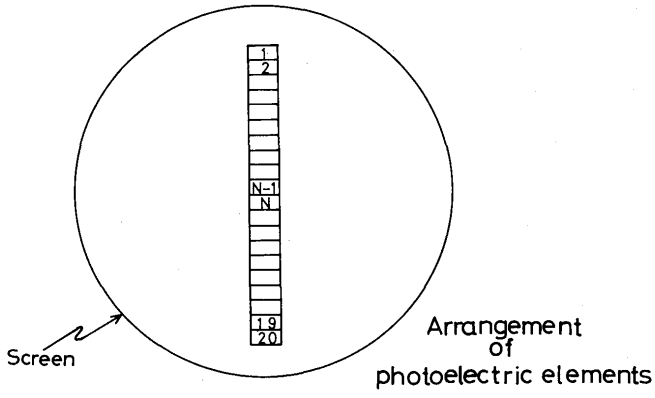

Fig. 4. Arrangement of photoelectric elements of the focussing screen.

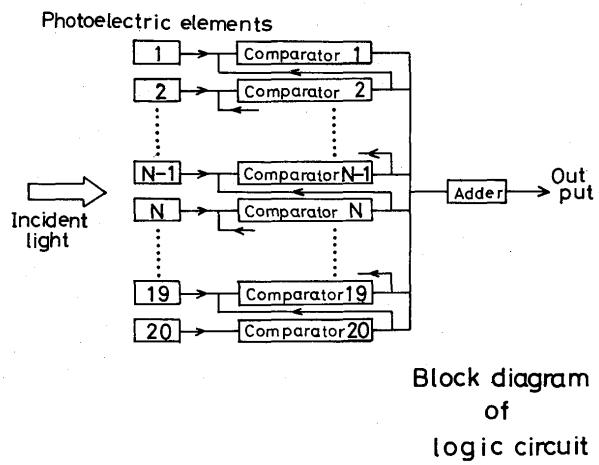

(a) Block diagram of the logic circuit.

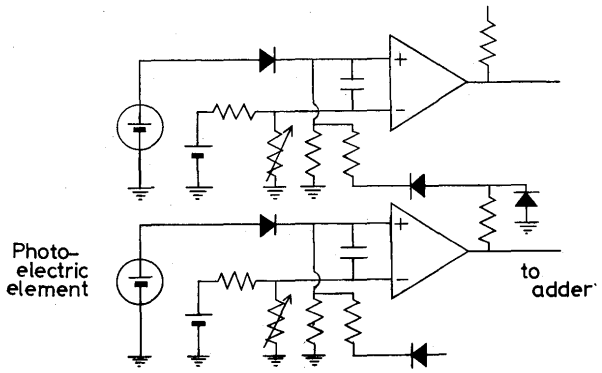

(b) Connection diagram of the voltage comparators.

Fig. 5.

voltage comparator is connected to the input terminal of the just beneath one, for instance, the output of the Nth voltage comparator is connected to the input of the (N-1)th comparator. All comparator outputs are also connected to the adder, thus, the adder output signal indicates the border position of the image.

If an incident light shines on the Nth photoelectric element, an electromotive force generates in such element and inverts the corresponding Nth comparator output level from low to high, hereby all the output levels of the (N−1) ~1th comparators are inverted from low to high, as a result, the adder output signal is proportional to N.

Figure 5 (b) shows the connection diagram of the voltage comparators.

Figure 6 shows an example of the output signal of the sensing device. The signal level changes according to the position change of the molten pool. The superposed ripple on the signal owes to fluctuation of the surface shape of the flowing molten metal. The ripple may be smoothed off by a conventional low-pass filter according to the purpose of the control.

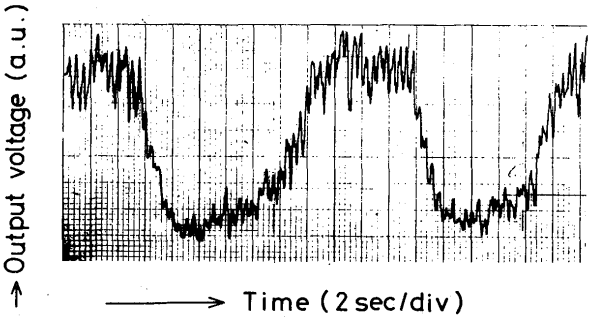

Fig. 6. One example of an output signal of the sensing device.

If a holizontal angle of the optical axis of the camera is proper, the image which is the same as shown in **Photo. 1** can be obtained. ($\varphi=20$, where φ is a holizontal angle). If not so, the obtained images become like those as shown in **Photos. 2 (a)** and **(b).**

Photograph 2 (a) is an example in the case where angle is too small ($\varphi=12$) and greater part of arc column are intercepted by the molten pool, and **Photo. 2 (b)** is an example where a holizontal angle is too large ($\varphi=30$) and the lower part of arc is in sight.

In both case, sensing the accurate position of the borders becomes difficult owing to deterioration of

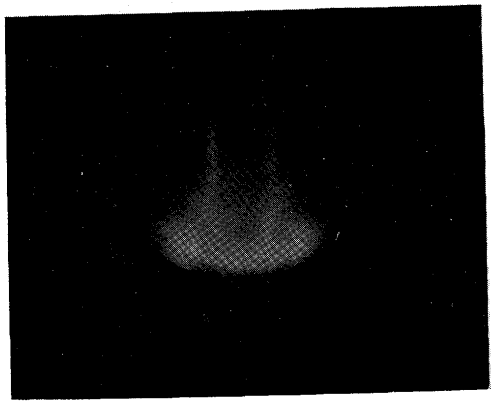

(a) A holizontal angle is too small.

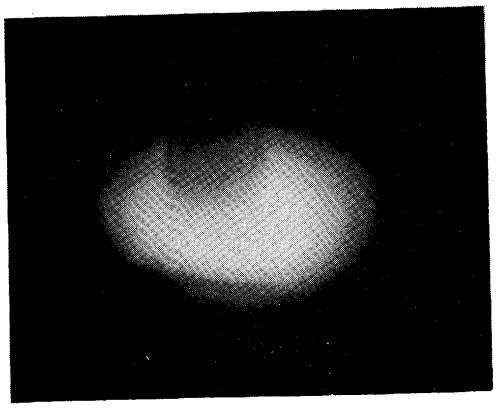

(b) A holizontal angle is too large.

Photo. 2. Various pattern of the image.

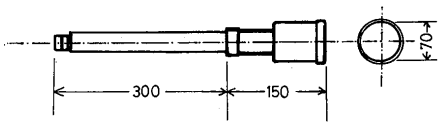

Fig. 7. Outside dimension of the camera.

S/N ratio of the image. The outside dimension of the camera is shown in **Fig. 7.** The camera is of 8.6 magnifications.

2-3 Static and dynamic properties of sensing device

The relation between the building up of the deposited metal and the sensing device output as a static property was investigated and dependence of the sensing ability on the various welding conditions was clarified by practical welding tests.

Welding tests were made in a CO_2 atomosphere on mild steel plates of square groove whose width was of 4～10 (mm). Arc power ranged from 225 (A) ～23 (V) to 450 (A) ～36 (V) and welding speed from 20 to 70, (cm/min).

All the other welding tests in the following sections were made under the same conditions as above. Effect of change in arc power on sensing ability was investigated. The result is shown in **Fig. 8,** where output voltage of the sensing device corresponding to a certain value of building up is plotted against arc power. From the figure, it is proved that arc power seldom effects on the sensing ability as the basis, but the measures of dispersion of the output signal increases slightly as arc power increases. In **Fig. 9,** the same output value as in **Fig. 8** is plotted against groove width of work pieces. The sensing ability does not depend on groove width.

Figure 10 shows the relation between output voltage of the sensing device and the sensed variable (so to say, controlled variable, the building up of the deposited metal) under various welding conditions. The experimental errors are within around 10 percent and have a tendency to converge to zero as the values approach to the origin, therefore, the accuracy of this sensing method is satisfactory in a feedback control system where a null method is usually used. The building up of the deposited metal after weld had been finished was measured with a conventional instrument composed of a dial gauge and two rollers as shown in **Fig. 11.**

The output signal of the sensing device has a slight time lag throughout all the experiments in this report, because a condenser is added parallel to each photoelectric element and forms a low-pass filter of CR circuit to smooth the output signal from the

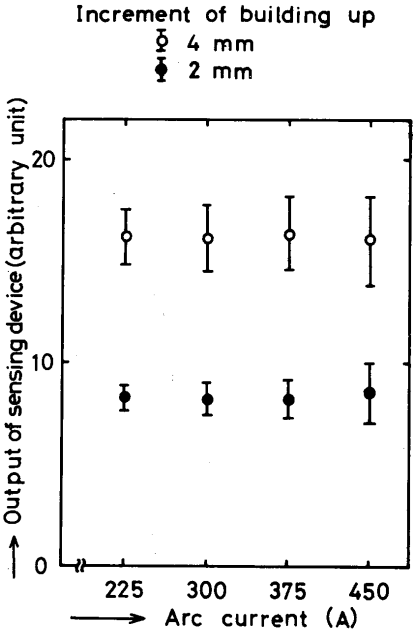

Fig. 8. Effect of arc power on sensing ability.

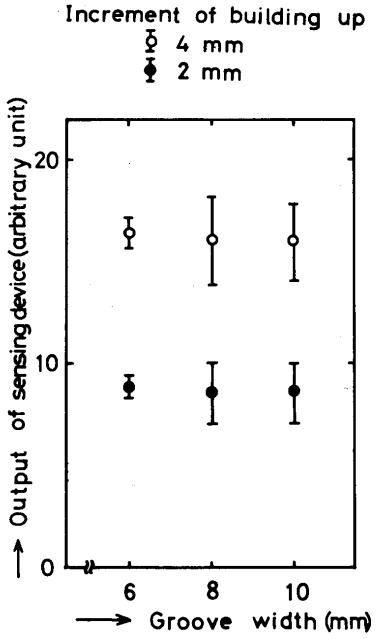

Fig. 9. Effect of groove width on sensing ability.

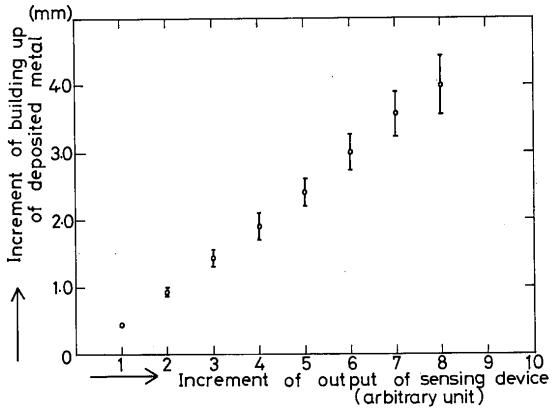

Fig. 10. Relation between output of the sensing device and sensed variable.

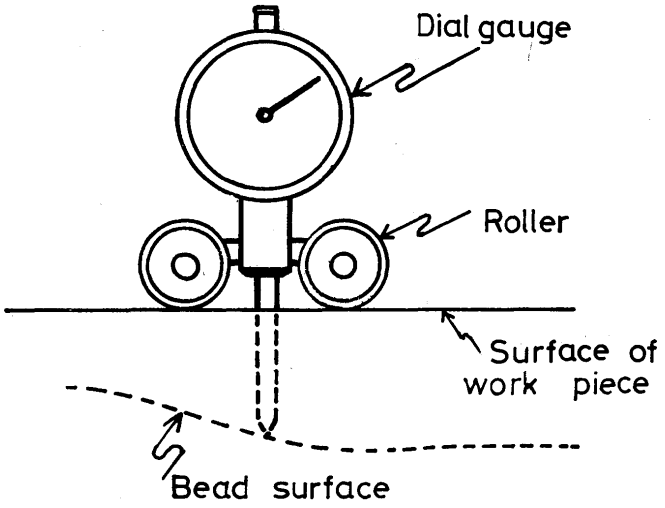

Fig. 11. Instrument for measuring building up.

photoelectric element.

The time constant of this CR circuit can be set to an appropriate value of negligible small accroding to the dynamic properties of the other elements in the system by adjusting capacitance of the condenser. The time lag is, therefore, negligible on the dynamic analysis of the system.

3. Static property of controlled system

Welds were made under the above mentioned conditions and the static relations between the manipulated variable (welding speed) and the controlled variable (building up of the deposited metal) were obtained. **Figure 12** shows them.

Experimental results at arc power 300 (A) ~ 30 (V), 375 (A)~34 (V) and 450 (A)~38 (V) are shown together with theoretical calculated results which are drawn with continuous curves. Theoretical calculation was made on the basis of the simple fact that the groove of the work piece is filled with feed wire metal only.

It is quite natural that the values plotted on the abscissa are inversely proportional to those on the ordinate, because the volume of the deposited metal per unit length along welding direction is inversely proportional to welding speed.

4. Dynamic property of controlled system

4-1 Experimental investigation of dynamic property

On the assumption that the controlled system was a first order system, the dynamic property was investigated by a step response method. In this method, the

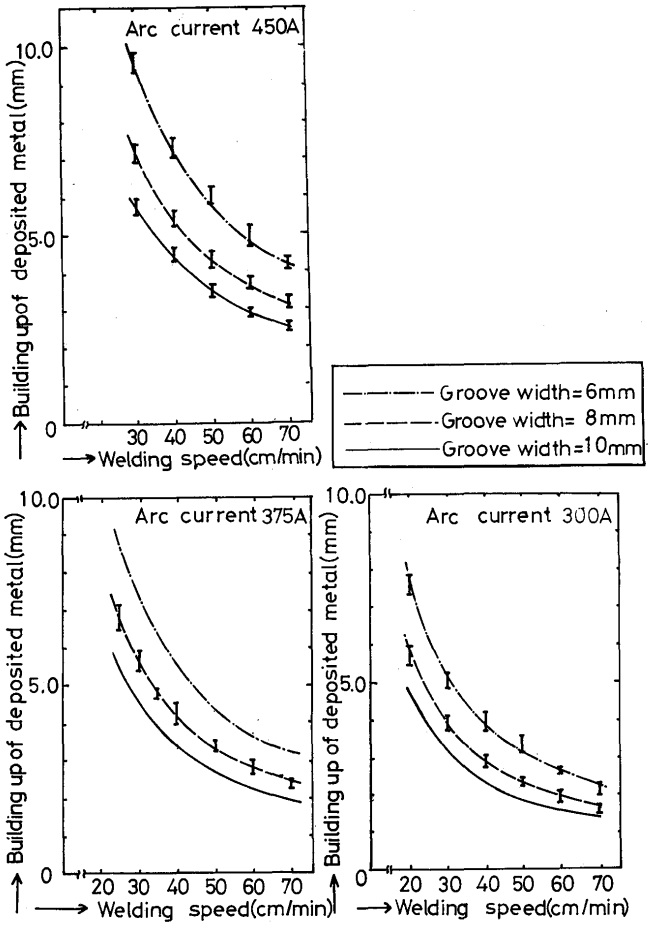

Fig. 12. Static relation between the manipulated variable (welding speed) and the controlled variable (building up of the deposited metal).

manipulated variable (welding speed) was changed in steps from v_1 to v_2, as shown **Fig. 13 (a),** (hereafter welding speed before and after change refer to v_1 and v_2 respectively) and the controlled variable (building up of the deposited metal) and its sensed value (the sensing device output) changed correspondingly as shown in **(b)** and **(c)** of **Fig. 13.**

A transient response of a first order system to a step input is formalized in the following equation.

$$Y(t) = Y_\infty \left\{ 1 - \exp\left(- \frac{t}{\tau} \right) \right\} \quad \cdots\cdots\cdots\cdots (1)$$

where Y(t) is a transient respones at a time t when a step whose magnitude is Y_∞ is applied at $t=0$ and τ is the time constant of the system. The experimental results were approximated by eq. (1).

In order to estimate the time constant from the transient response curve of the sensing device output, the response value y_i at a time t_i ($i=1\sim n$) sampled from the curve was plotted on semilog paper with time on the linear scale where the response y_i was sampled

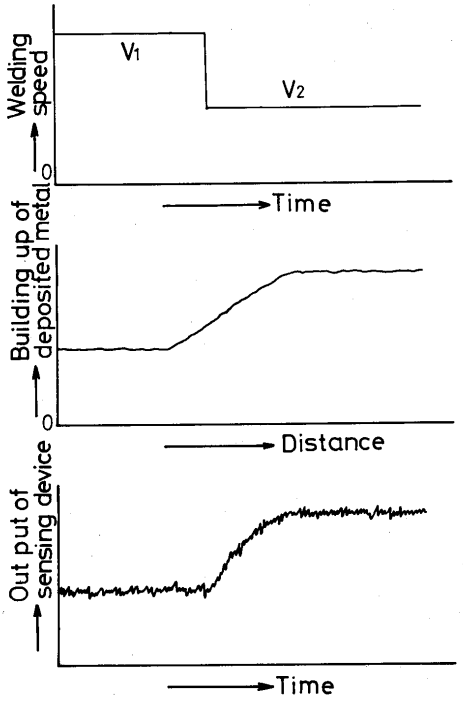

Fig. 13. Step response of the controlled system.

so that $y_i \to 0$ at $t_i \to t_n (i \to n)$ as shown in **Fig. 14.** From the fact that a first order system with a time constant τ gives a linear response and the slope of this line is the reciprocal of τ, i. e.

$$\frac{\Delta \log_{10} y}{\Delta t} = \frac{\log (y_i / y_j)}{t_i - t_j} = \frac{0.434\cdots}{\tau} \quad (i \neq j) \qquad \cdots\cdots (2)$$

where i and j are arbitrary within the limit on n, τ can be obtained on using a least square method. Sampling was made on so many data of y_i $(i=1 \sim n)$ as that enough reliability on the τ value could be assured.

Welding speed was changed by controlling the aplaying voltage to the armature of the carriage motor.

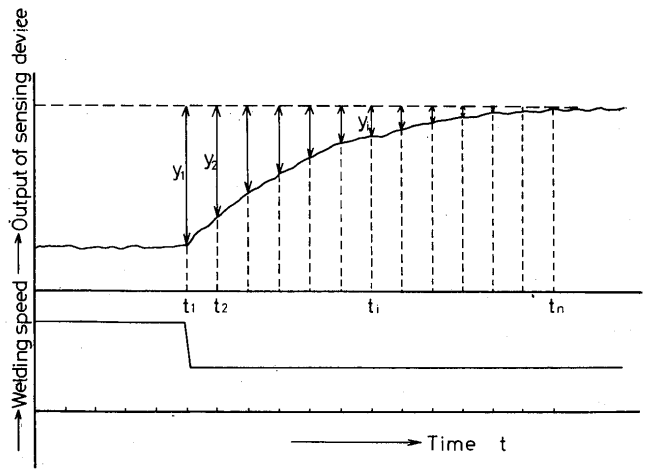

Fig. 14. Sampling of y_i from a transient response curve.

The connection diagram of the control circuit for the carriage motor is shown in **Fig. 15.** The relay R acts by closing the switch SW , the external resistance of the symmetrical thyristor unit is switched over from r_1 to r_2, and the firing phase of the thyristor changes, as a result, the DC voltage applied to the armature changes in steps. At the same time, the relay R acts, and the light emitting diode is connected to the DC power source and generates the light signal.

In the practical welding experiments, the change of welding speed is not in steps, but has time lag, because the transient response of the carriage motor speed to a step change of armature voltage is of first order and follows eq. (1). Therefore, strictly speaking, the transient response of the sensing device is of the second order, and it must be modified by the following first order system equation

$$\tau_M \frac{dY(t)}{dt} + Y(t) = Z(t) \qquad \cdots\cdots (3)$$

where τ_M is the time constant of the carriage motor and Y(t) is the original response and Z(t) is the modified to which time lag compensation has been made.

On obtaining τ practically, z_i and z_j were substituted into eq. (2) instead of y_i and y_j, where z_i (and z_j, too) could be calculated out from eq. (4) which was derived from eq. (3) by the simplest finite defference approximation.

$$\tau_M \frac{y_{i+1} - y_i}{t_{i+1} - t_i} + y_i = z_i \qquad \cdots\cdots (4)$$

The relation among Y(t), Z(t), y_i and z_i is shown in **Fig. 16.** The time constant τ_M was measured in the experiment previously made and ranged from 0.2 to 0.4 (sec) depending on v_1 and v_2.

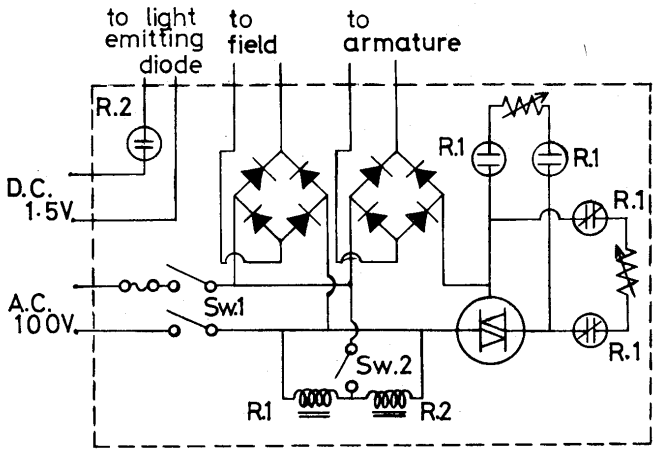

Fig. 15. Connection diagram of the control circuit for the carriage motor.

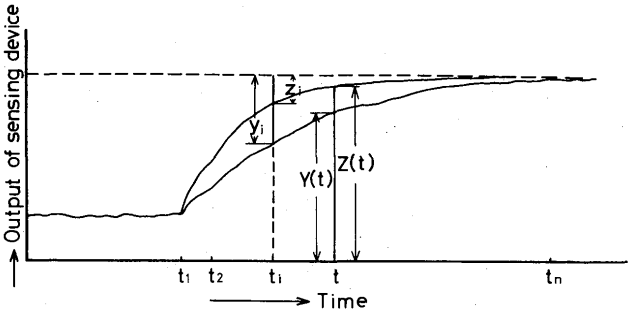

Fig. 16. Relation among Y(t), y_i and their modified values Z(t), z_i.

4-2 Experimental results

An example of the experimentally obtained τ value which is plotted against increment of welding speed $\Delta v(=v_2-v_1)$ is shown in **Fig. 17** where the welding condition is described. The plot is made for constant v_2 for several values of v_2. The τ value is constant and does not depend on Δv for $\Delta v<0$, but depends on Δv for $v>0$ and increases gradually as Δv increases. The values of τ which were obtained under the other various welding conditions show a similar tendency as shown in **Fig. 18.**

The τ value which is defined in the following equation is required in order to compose an automatic feedback control system.

$$\tau_0 = \lim_{\Delta v \to 0} \tau(\Delta v) \quad \cdots\cdots (5)$$

Values of τ_0 were obtained in practice by graphical interporation from **Figs. 17** and **18. Figures 19** and **20** are plots of τ_0 versus v_2 for the constant welding condition for several conditions.

It is proved that arc power effects on τ_0 versus v_2 curves as is seen in **Fig. 19** (in this figure, parameter is expressed in arc current instead of arc power), but

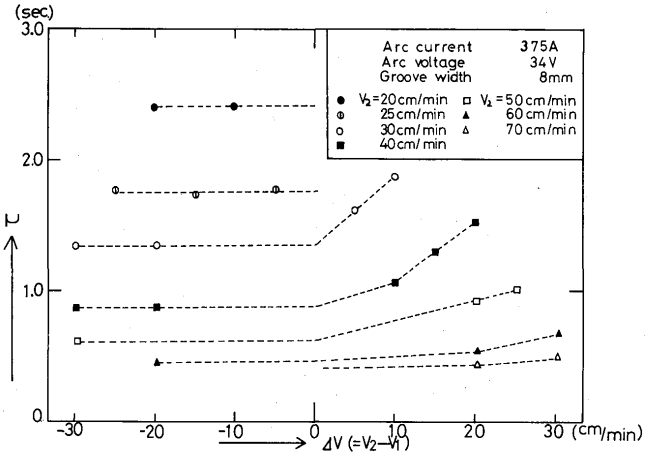

Fig. 17. Relation between τ and Δv.

groove width of the work piece does not effect as is seen in **Fig. 20.** An experimental equation on τ_0 was obtained from these results as follows.

$$\tau_0 = \frac{9.11}{v} - \frac{45.6}{I^{0.772}} \quad \cdots\cdots (6)$$

where τ_0 is in (sec), v is in (mm/sec) and I is arc current in (A).

4-3 Supplementary experiments and their results

A few supplementary experiments were made for explanation of the values of τ and τ_0, and their properties. The experiment to obtain the shape and the size of the molten pool by an impact method in expectation that there might exist any relations between the values τ, τ_0 and them.

In this method, a sudden impact was applied to the work piece during welding with the apparatus as shown in **Fig. 21,** the existing molten metal in a pool was driven out in a moment and the shape of the solidus interface was well preserved.

Figures 22 and **23** show the longitudinal sections of the preserved solidus interface. It results from **Fig. 22** that the groove width of the work piece does not effect on the shape and the size of the molten pool within the experimented range. The fact that the groove width does not effect the τ_0 value can be explained by this results. **Figure 23** shows the longitudinal sections for various values of welding speed. The length of the molten pool measured from these sections does not depend on welding speed. **Figure 24** also shows this fact, where the length is plotted against welding speed, but the length is effected by arc current.

The experiment to observe the behavior of the molten metal at the moment of the welding speed change was made to investigate dependency of τ on Δv. L-shaped wires of diameter 2 (mm) were sets in the hole drilled at the bottom of the groove of the work piece as shown in **Fig. 25** and weld was made. The welding speed change during welding was made at the Ni wire set position from v_1 to v_2 for the various of v_1 and the constant value of v_2. After welds had been finished, the work pieces were cut at their longitudinal sections and macro etched to clarify the molten Ni flow pass.

Photograph 3 shows the macro-etching results. In all cases, Ni flows forward from the welding speed changed position and this indicates the contribution of some parts of the molten metal at speed v_1 to the formation of the molten pool at speed v_2, but in the case for $\Delta v<0$, i.e. $v_1>v_2$ and the building up gradually increases after the speed change, the flow rate is kept constant and nearly equal to the case of constant

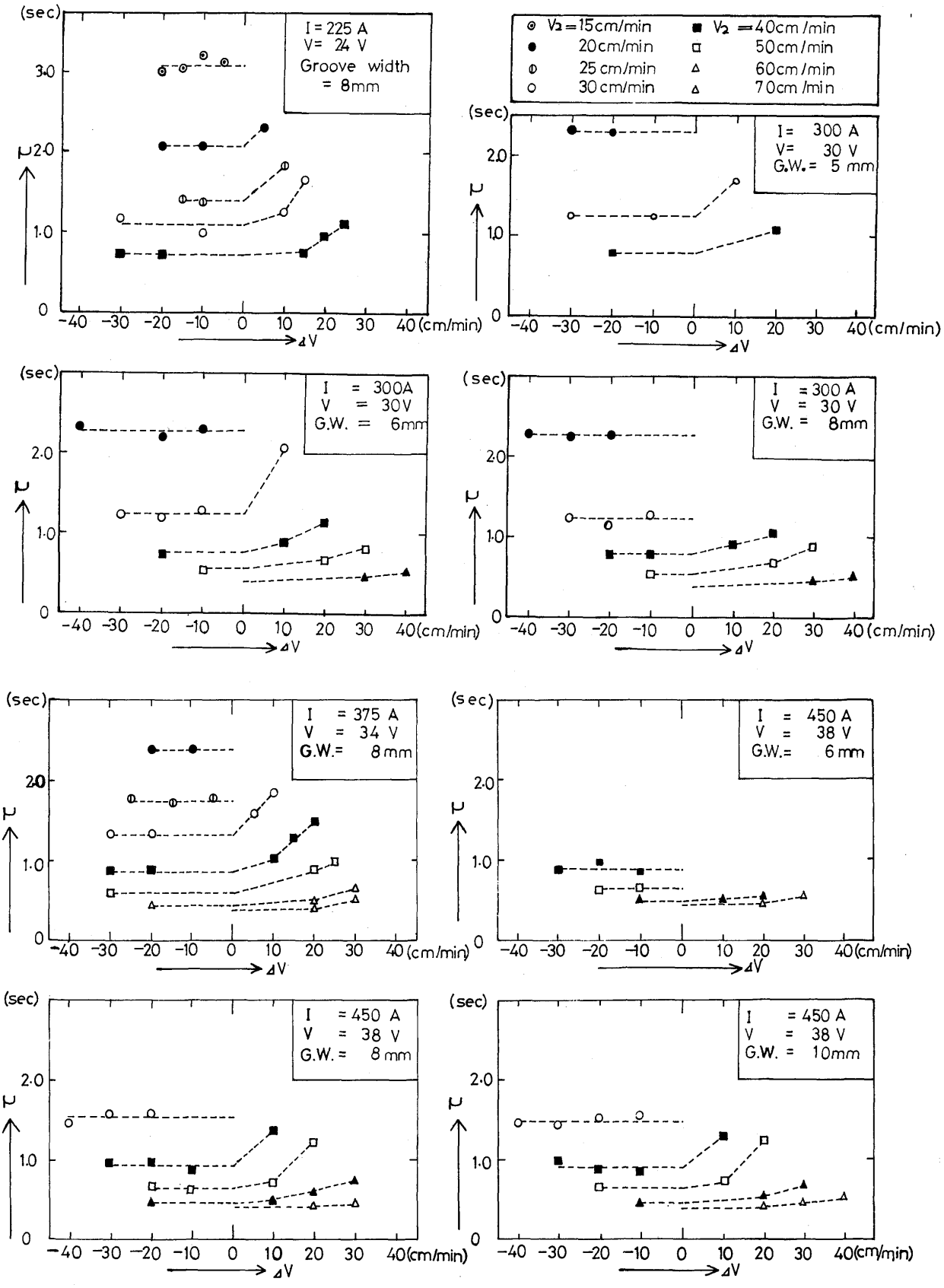

Fig. 18. Relation between τ and Δv.

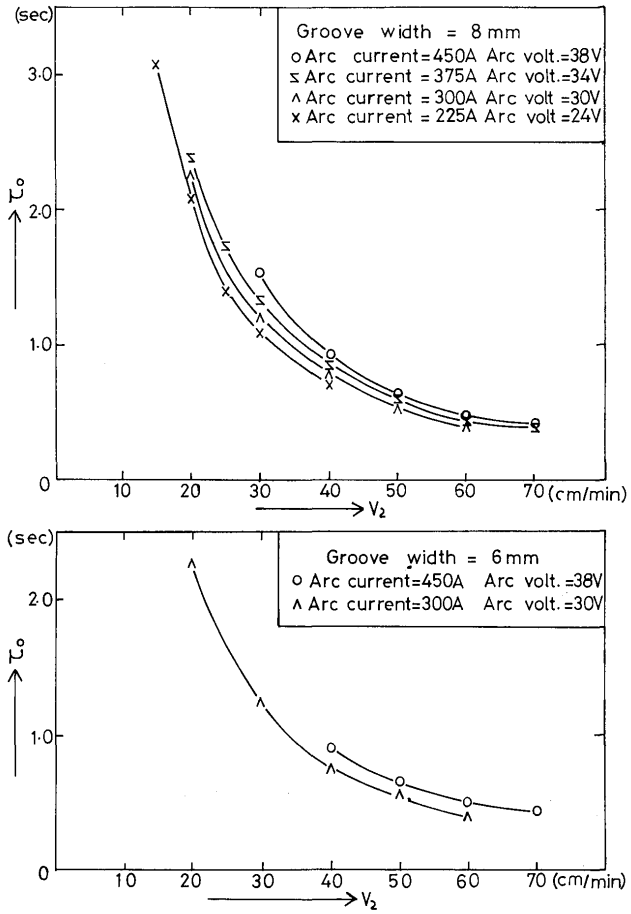

Fig. 19. Relation between τ_0 and v_2 where parameter is arc current.

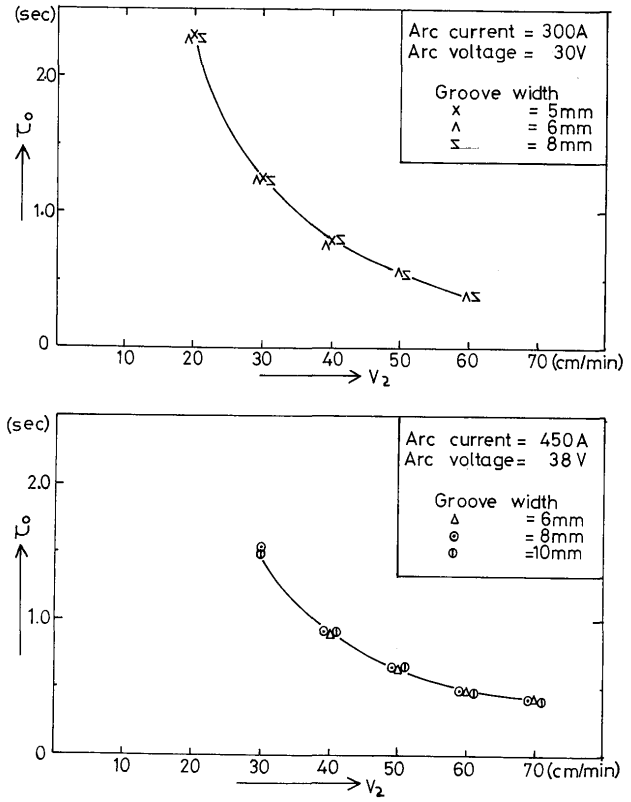

Fig. 20. Relation between τ_0 and v_2 where parameter is groove width of the work piece.

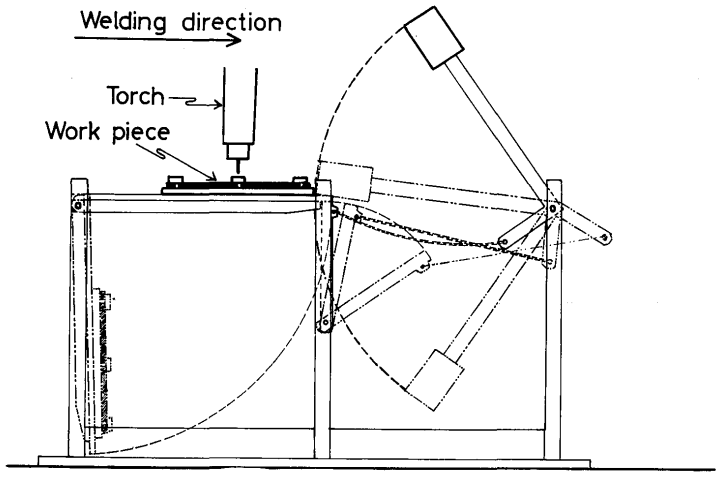

Fig. 21. Impacting apparatus for work piece.

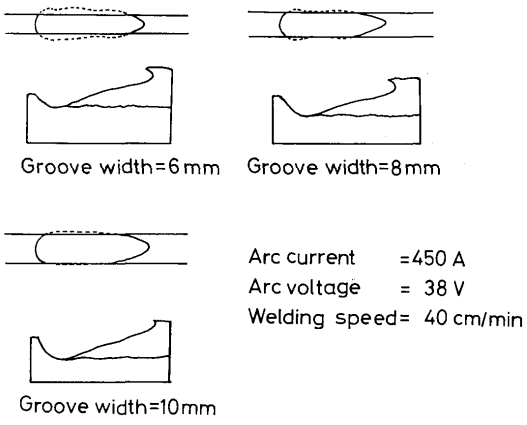

Fig. 22. Section of the molten pool.

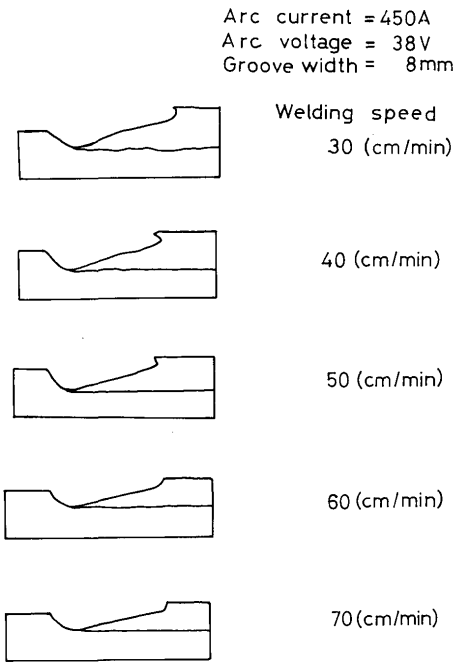

Fig. 23. Longitudinal section of the molten pool.

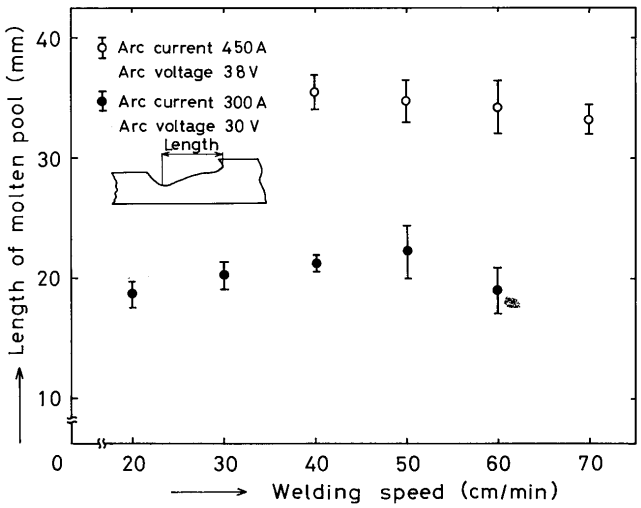

Fig. 24. Relation between welding speed and length of the molten pool.

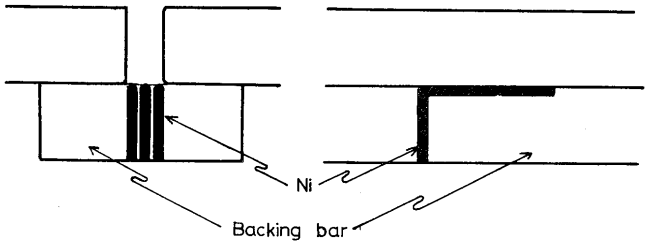

Fig. 25. Setting of L-shaped Ni wires at the work piece.

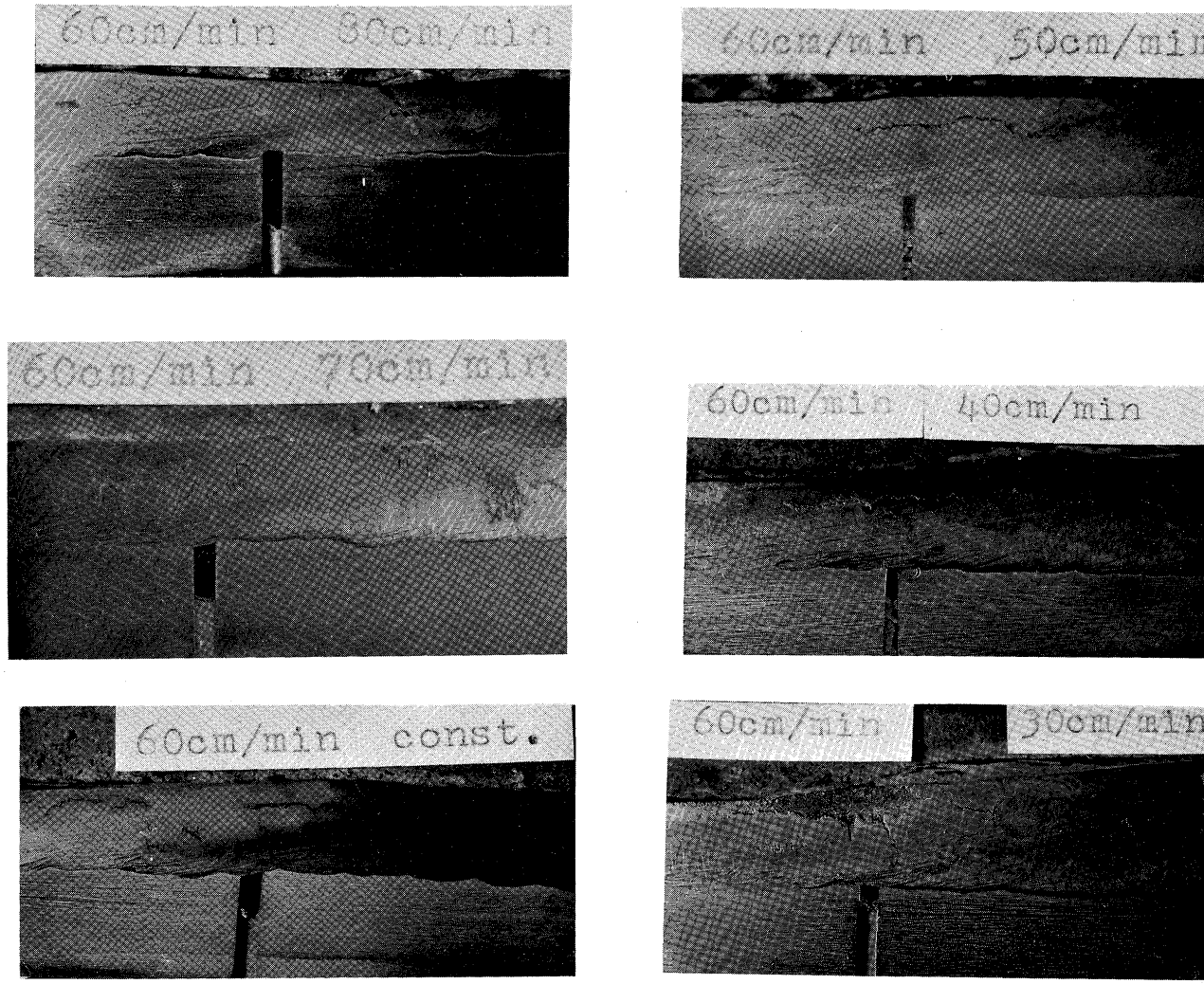

Photo. 3. Macro-etched longitudinal section of the work piece.

welding speed, while in the case for $\Delta v > 0$, the flow rate increases as Δv increases as observed from **Photo. 3.**

It can be well explained from these results that, in the case building up increases, τ is kept constant because contribution degree of the molten metal having existed in the pool before the welding speed change to the formation of the molten pool after the speed change does not depend on the increment of the speed Δv and is kept nearly constant, on the other hand, in the case building up decreases, this contribution degree depends on Δv and increases with it. And this means that more time is required to attain the steady state after the speed change. The dependency of τ on Δv as described about **Figs. 17** and **18** can be well explained by the abovementioned fact.

4-4 Consideration and Discussion

Let us consider theoretically the reason why the time lag generates in the building up phenomena. For theoretical consideration, we assume the upper part of the longitudinal section of the molten pool as a rectangular shape as shown in **Fig. 26 (a),** where L is the effective length of the molten pool, h is the height of the building up. We also assume that the effective length L is kept constant during welding independently of welding speed. This assumption is seemed to be proper from the result of the previous section.

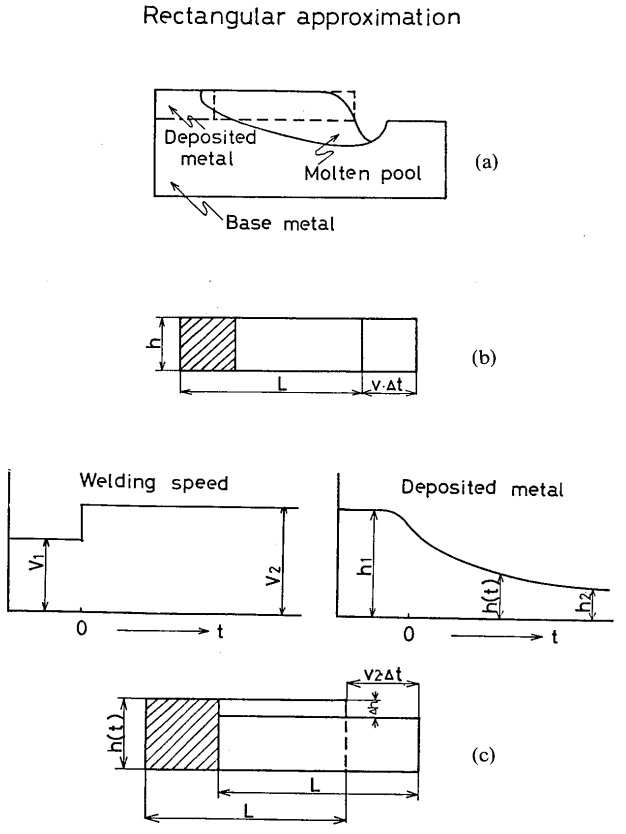

Fig. 26. Rectangular approximation of the molten pool.

When weld is made with welding speed v and wire feed rate F, the transfer distance of the molten pool in a period of Δt is $v \cdot \Delta t$, the solidificated volume of the molten metal is $h \cdot v \cdot \Delta t$ and the transfered volume of the metal from the feed wire to the work is $F \cdot \Delta t$ in this period, therefore, in a steady state

$$(F - v \cdot h) \cdot \Delta t = 0 \quad \text{or} \quad F = v \cdot h \qquad \cdots\cdots (7)$$

as shown in **Fig. 26 (b).**

If welding speed changes suddenly from v_1 to v_2 in steps at a time $t=0$. h begins to change gradually from the initial steady state value h_1 to the final one h_2 The incremental value Δh of h(t) in a small period at a time t is then

$$\Delta h(t) = -\frac{1}{L}\left\{ v_2 \cdot h(t) - F \right\} \cdot \Delta t \qquad \cdots\cdots (8)$$

as shown in **Fig. 26 (c),** where $L \cdot \Delta h$ corresponds to the volume increment of the molten pool.

The limitting form of eq. (8) as $\Delta t \to 0$ is the following first order differential equation.

$$L\frac{dh(t)}{dt} + v_2 \cdot h(t) - F = 0 \qquad \cdots\cdots (9)$$

Solving eq. (9), substituting the steady state condition: $F = v_2 \cdot h_2 = v_1 \cdot h_1$(i. e. eq. (7)) and the initial condition; $t=0$, $h(t) = h(0) = h_1$, and rearranging, we obtain,

$$h(t) = (h_2 - h_1)\left\{ 1 - \exp\left(-\frac{v_2 \cdot t}{L} \right) \right\} + h_1 \qquad \cdots (10)$$

Comparing eq. (10) with eq. (1), we can get as the time constant

$$\tau = \frac{L}{v_2} \qquad \cdots\cdots (11)$$

While, eq.(6) can be rewritten as follows

$$\tau_0 = \frac{a}{v} - b \qquad \cdots\cdots (6')$$

where a is constant and b is also constant if arc power is constant. The from of eq. (6′) is different from that of eq. (11). The former was obtained experimentally and the latter was theoretically. We ventured two hypotheses to explain the difference. One of them is that the effective length of the molten pool L in eq. (11) corresponds to L_2 which can be calculated by the following equation that is derived from eq. (6)

$$\left.\begin{aligned} L_2 &= L_1 - L_1' \\ L_1 &= a \\ L_1' &= b \cdot v \end{aligned}\right\} \quad \tau_0 = \frac{L_2}{v} \qquad \cdots\cdots (6'')$$

that is to say, the effective length is not constant in eq. (6″), (and therefore in eq. (6)), but decreases

linearly with welding speed.

The other hypothesis is that eq. (6′) again rewritten as follows

$$\left.\begin{matrix} L_1 = a \\ \tau_0' = b \end{matrix}\right\} \rightarrow \tau_0 + \tau_0' = \frac{L_1}{v} \quad \cdots\cdots (6''')$$

This equation means that the experimental τ_0 is slightly less than the theoretical time constant. This is due to the reason that the measurement of τ_0 is made to the molten pool which responses more quickly than the molten pool in the the theoretical consideration where its average behavior is discussed.

Figure 27 shows the ratio L_0/L_1 and L_0/L_2, where L_0 is the measured length of the molten pool which was plotted on orginate in **Fig. 24,** L_1 and L_2 is described in eqs. (6″)and (6‴). In this figure, L_0/L_2 is effected by welding speed and increases with it while L_0/L_1 is kept constant. The latter hypothesis is seemed to be proper from this fact. The values of the time constant difference τ_0' versus arc current are shown in **Table. 1.** It may be allowable that there exists the difference of such degree in the time constant between the experimental result and the theoretical one.

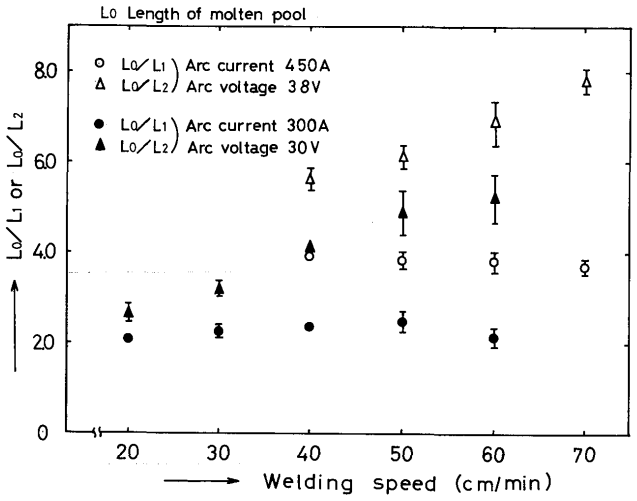

Fig. 27. Relation between welding speed and L_0/L_1 or L_0/L_2.

Table 1. Values of the time constant difference τ_0' versus arc current.

Arc current (A)	225	300	375	450
τ_0' (sec)	0.70	0.54	0.48	0.41

5. Automatic control experiment

5-1 Composing of feedback control system

The parameters of the controlled system are effected by the input to it as mentioned in the previous sections. That is to say, when we assume the controlled system as first order and expresses its transfer function as follows (this expression itself has already been self-contradictory),

$$G_s(s) = \frac{K_1}{1+\tau \cdot s} \quad \cdots\cdots (12)$$

the parameters, k_2 and τ depend on the manipulated variable (welding speed) v, and vary with it. Strictly speaking, an optimum control theory where the system is described by state vectors must be used for analysis and synthesis on such system.[6)~8)] However, it is sufficient to use a theory for a linear and stationary system where application of Laplacian transformation and describing a system by a transfer function are possible in order to analize the system approximately, because the automatic control experiment was performed only to verify the properties of the sensing method and the obtained τ_0 value qualitatively.

Based on above premise, the automatic feedback control system was composed as shown in **Fig. 28,** where notation is as follows:

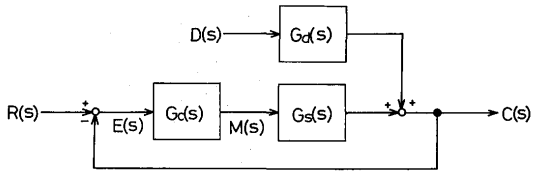

Fig. 28. Block diagram of the automatic feedback control system.

$G_s(s)$: controlled system
$G_c(s)$: control element
$G_d(s)$: disturbance transfer element
$G_f(s)$: feedback element
R (s): reference
E (s): actuating signal
M (s) manipulated variable
D (s): disturbance
C (s): controlled variable

The transfer function of the controlled system was already described in eq. (12). The control element is composed of an integrator, a servo-amplifier and a carriage motor as shown in **Fig. 29.** This is the third or much higher order system to be exact, but because the function of the integrator is dominant in a transient state and the time lag of the other elements than the integrator is a negligible amount, the transfer function of the control element was assumed to be of an integral element as follows:

$$G_c(s) = \frac{K_2}{s} \quad \cdots\cdots (13)$$

The time lag of the feedback element (the sensing device) is also negligible as mentioned, and its transfer function is

$$G_f(s) = 1 (= \text{constant}) \quad \cdots\cdots (14)$$

Fig. 29. Block diagram of the control element.

The reference does not change during welding, therefore

$$R(s)=0 \rightarrow C(s)=-E(s) \quad \cdots\cdots (15)$$

Thus, we can obtain the relation between the controlled variable C (s) and the disturbance D (s) as follows:

$$C(s)=\frac{G_d(s)}{1+G_f(s)\cdot G_c(s)\cdot G_s(s)}\cdot D(s)$$

$$=\frac{G_d(s)}{1+\frac{K_1\cdot K_2}{s(1+\tau\cdot s)}}\cdot D(s)$$

$$=\left(1-\frac{\frac{K}{\tau}}{s^2+\frac{s}{\tau}+\frac{K}{\tau}}\right)\cdot G_d(s)\cdot D(s)$$

$$=G_w(s)\cdot D(s) \quad \cdots\cdots (16)$$

where $K=K_1\cdot K_2$

5-2 Disturbance and disturbance transfer function

A change of the groove width of the work piece was supposed as the disturbance to the system. The change was in steps and in ramps.

Then, it is expressed

$$D(s)=\frac{1}{s} \text{ or } \frac{1}{s^2} \quad \cdots\cdots (17)$$

Weld was made on such work and the time constant τ of the sensing device output was investigated by the same method as the case of welding speed change.

Figure 30 shows an example of the weld result. The time constant τ is also effected by welding speed and is reciprocals of it

$$\tau_d=\frac{12.2}{v} \quad \cdots\cdots (18)$$

where v is in (mm/sec). The disturbance transfer function is expressed as first order

$$G_d(s)=\frac{K_3}{1+\tau_d\cdot s} \quad \cdots\cdots (19)$$

5-3 Transient behavior of the system

Substituting eqs. (17) (D (s) $=\frac{1}{S}$) and (19) into eq. (16), we obtain eq. (20) as a step response of the system.

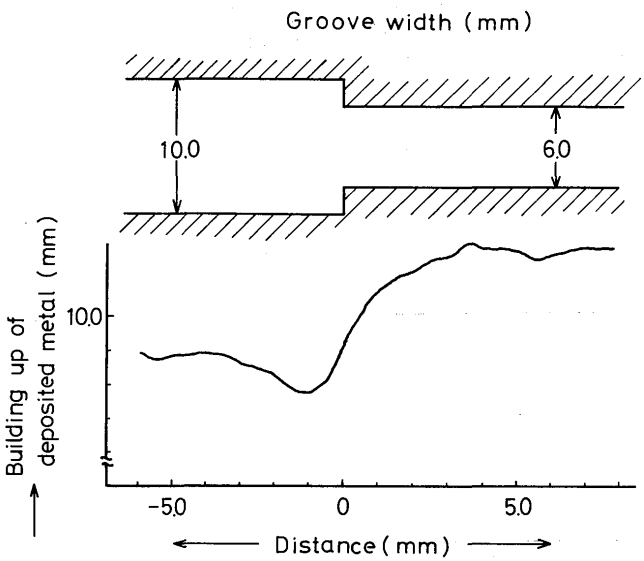

Fig. 30. Example of disturbance to the system.

$$C(s)=\left(1-\frac{\frac{K}{\tau}}{s^2+\frac{s}{\tau}+\frac{K}{\tau}}\right)\frac{K_3}{1+\tau_d\cdot s}\cdot\frac{1}{s} \quad \cdots (20)$$

Performing reverse Laplasian transformation of C(s), the transient behavior of system is obtained as a function of time.

$$C(t)=-E(t)=L^{-1}(C(s))$$

$$=K_3\cdot\left[-e^{-\frac{t}{\tau_d}}+|A(s_1)|\cdot e^{\frac{\zeta}{\sqrt{1-\zeta^2}}\angle A(s_1)}\right.$$

$$\cdot\frac{1}{\sqrt{1-\zeta^2}}\cdot e^{-\zeta\omega_n\left\{t+\frac{\angle A(s_1)}{\sqrt{1-\zeta^2}\omega_n}\right\}}$$

$$\cdot\sin\left\{\sqrt{1-\zeta^2}\,\omega_n\left(t+\frac{\angle A(s_1)}{\sqrt{1-\zeta^2}\,\omega_n}\right)\right.$$

$$\left.\left.+\tan^{-1}\frac{\sqrt{1-\zeta^2}}{\zeta}\right\}\right] \quad \cdots\cdots (21)$$

where $\omega_n=\sqrt{\frac{K}{\tau}}$

$$\zeta=\frac{1}{2}\sqrt{\frac{1}{\tau\cdot K}}$$

$$A(s)=\frac{1}{1+\tau_d\cdot s}$$

$$s_1=-\zeta\cdot\omega_n+j\sqrt{1-\zeta^2}\cdot\omega_n$$

The behavior of C(t) to t depends on ζ as shown in **Fig. 31.** The values of ζ must be set properly within the region of 0.4~0.6 in order to make the system well behave in a transient state.

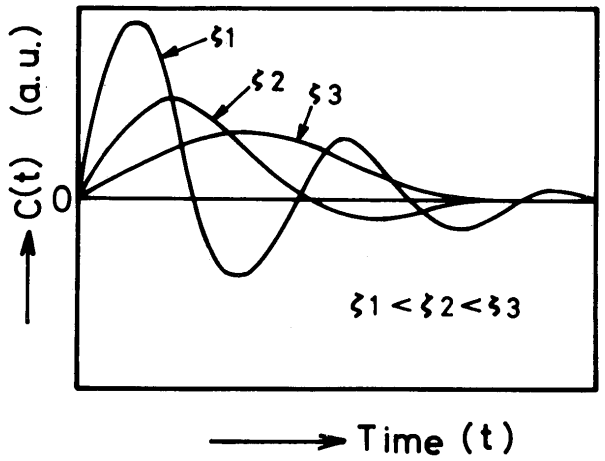

Fig. 31. Theoretically calculated transient response of the controlled variable in the feedback system and effect of the value ζ on it.

5-4 Examples of automatic control experiment

Figure 32 shows an example of the automatic feedback control experiment, where weld was made on the work piece whose groove width changed in steps as illustrated in the figure under the described welding condition. The broken line of the graph in the figure corresponds to the case without feedback control. The value ζ was set in 0.5 in this experiment. Comparison of the experimentally measured controlled variable with theoretically calculated result from eq.(21) is shown in **Fig. 33.** They are well agreed with.

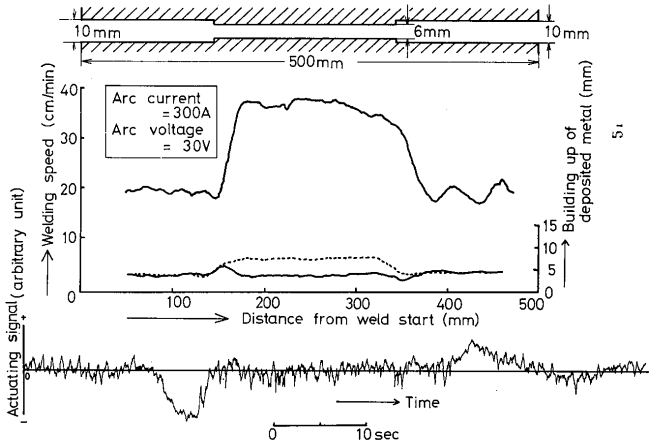

Fig. 32. Result of the automatic control experiment.

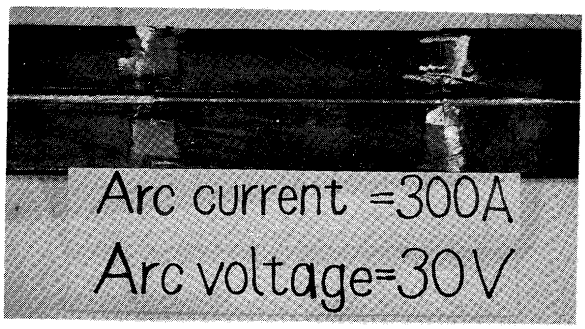

Photo. 4. Appearance of the automatic control welded work piece.

Photograph 4 shows an appearance of the work piece on which the experiment was made.

Figure 34 shows another example of the control where the groove width changes in ramps. The result is more satisfactory than the fomer example.

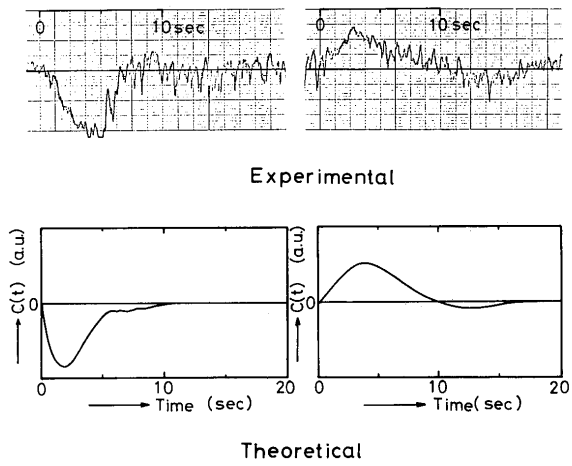

Fig. 33. Comparison of the experimental transient response with theoretical.

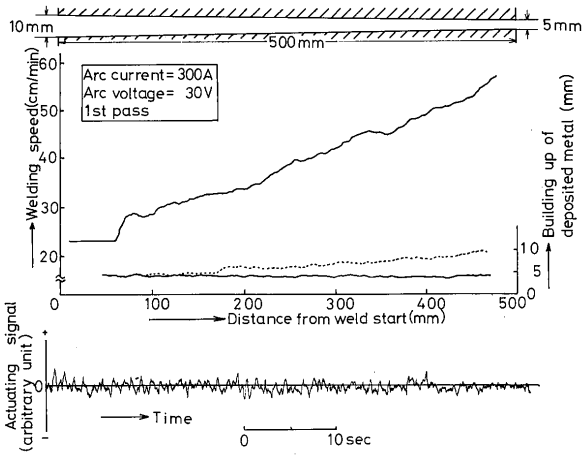

Fig. 34. Result of the automatic control experiment.

6. Conclusion

1. A new controlled variable other than penetration was developed in an automatic control system of arc welding.
2. The sensing method for this controlled variable was established. Its accuracy was tested experimentally and verified to be satisfactory for using it in a feedback system.
3. Static property of the controlled system for this controlled variable was investigated experimentally and well coincide of the experiment with a theory was recognized.
4. Dynamic property of the controlled system was

investigated experimentally by a step response method on assumption of the first order system, and the time constant of the system was obtained. This time constant is remarkable effected by welding speed and slightly by arc current. Experimental equation was obtained from these results.

5. Theoretical consideration on the time constant was made, and comparison of the theoretical consideration with the experimental result was also made. The difference between both was well explained by a ventured hypothesis.
6. Automatic control experiments were made in order to verify the investigated properties of the sensing method, the controlled system and the controlled variable, qualitatively. Their results are satisfactory.
7. It is a subject in the next step to synthesize the much better automatic feedback control system on using an optimum control theory based on the properties investigated in this study.

References

1) P. W. Ramsey, J. J. Chyle, J. N. Kuhr, P. S. Myers, M. Weiss and W. Groth: "Infrared Temperature Sensing Systems for Automatic Fusion Welding", W. J., (1963), No. 8, 337s～346s.
2) E. P. Vilkas; "Automation of Gas Tungsten-Arc Welding Process", W. J., (1966), No. 5, 410～415s.
3) N. S. L'vov: "Automation of Arc Welding of Means of Integrated Control Systems" Weld Prod., (1969), No. 6, 10s～12s.
4) W. M. McCompbell, G. E. Cook, L. E. Nordholt and G. J. Merrick: "The Development of a Weld Inteligence System", W. J., (1966), No. 3, 139s～144s.
5) "System Maintains Constant Weld Penetration", W. Eng., (1967), No. 11, 59s.
6) R. Bellman: "Adaptive Control Process", Princeton University Press, (1961).
7) Pontryagin, Boltyanskii, Gamkrelidze and Mishchenko: "The Mathmatical Theory of Optimal Processes", Intercience (1962).
8) J. I. Tou: "Modern Control Theory", McGraw-Hill (1964).